

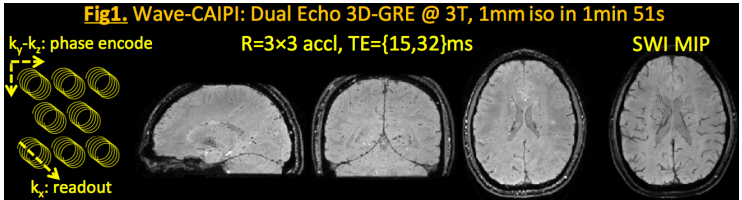
# Accelerated QSM

Berkin Bilgic<sup>1</sup>, Stephen F Cauley<sup>1</sup>, Huihui Ye<sup>2</sup>, Christian Langkammer<sup>3</sup>, Benedikt A Poser<sup>4</sup>, Kawin Setsompop<sup>1</sup>

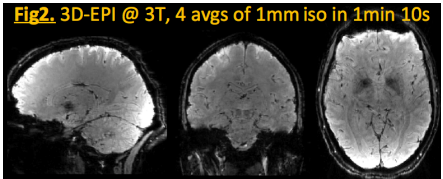
<sup>1</sup>Martinos Center, Massachusetts General Hospital, Charlestown, MA, USA; <sup>2</sup>Center for Brain Imaging Science and Technology, Zhejiang University, Hangzhou, China; <sup>3</sup>Department of Neurology, Medical University of Graz, Graz, Austria; <sup>4</sup>Department of Cognitive Neuroscience, Faculty of Psychology and Neuroscience, Maastricht University, Netherlands.

**INTRODUCTION:** SWI and QSM harness the tissue magnetic susceptibility as a contrast mechanism for detailed depiction of the vasculature, deep gray matter and the cortex. The tissue susceptibility is derived from the phase of the GRE signal, which attains maximum contrast-to-noise ratio when the TE is equal to the tissue  $T_2^*$  relaxation time. Due to long TE and whole brain coverage requirements, SWI and QSM acquisition using conventional 3D-GRE is relatively slow. When coupled with multiple head orientation requirement of COSMOS [1] and STI [2], the scan time becomes prohibitively long. As the SNR benefit of ultra high field permits smaller voxel sizes, acquisition time remains relatively long despite the reduction in the optimal  $TE=T_2^*$ . To reduce the scan time, it is possible to employ (a combination of) *i*) parallel imaging acceleration, *ii*) efficient k-space trajectory, and *iii*) echo-shift to exploit the unused sequence time due to long TE. In this abstract, we review and provide examples for each category.

**METHODS&RESULTS:** *i*) **Parallel imaging:** uses coil sensitivity encoding to reconstruct data from undersampled acquisitions. Since 3D-GRE entails phase encoding in both  $k_y$  and  $k_z$  axes, acceleration in two dimensions becomes feasible. This has been employed for  $R=2\times 2$ -fold speed-up using GRAPPA [3,4], and  $R=2.5\times 2$ -fold acceleration with SENSE [5,6]. Parallel imaging performance can be improved using 2D-CAIPI [7], which controls the voxel aliasing pattern by shifting the position of k-space samples. Aliasing can also be distributed along the fully-sampled  $k_x$  axis, which further improves parallel imaging and forms the basis of Wave-CAIPI [8]. As shown in **FIG1**, this allows  $R=3\times 3$ -fold acceleration with high image quality, where two flow-compensated echos were sampled for improved SNR in 1min 51s. Image reconstruction was performed online and helical k-space trajectory was estimated automatically from the undersampled data [9].

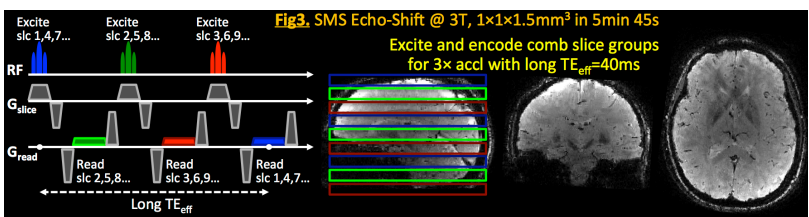


*ii*) **Efficient trajectories:** **EPI** covers a plane of  $k_x-k_y$  per excitation, making it an efficient tool for phase imaging. Single-shot 2D-EPI allows whole brain coverage at 2mm isotropic resolution in 7s [10], and can be further sped up using Simultaneous MultiSlice (SMS) [11]. 3D-EPI [12] follows an EPI trajectory for in-plane sampling, with phase encoding along the  $k_z$  axis. This results in an efficient encoding strategy with the SNR benefit of 3D signal averaging. **FIG2** demonstrates a whole brain 3D-EPI acquisition at 1mm isotropic resolution, which took 1min 10s for 4 averages. This acquisition used  $R=3$ -fold GRAPPA acceleration to reduce distortion. Segmented EPI is another strategy that mitigates distortion by covering the  $k_x-k_y$  plane in multiple excitations. Combined with the SNR efficiency of 3D encoding, this allows a 4min acquisition at 0.55mm isotropic resolution with low distortion [13]. 2D-CAIPI is also applicable to 3D-EPI, which permits high acceleration rates to interchangeably achieve faster acquisition or reduced distortion [14,15].



**PROPELLER** collects low-resolution data strips, aka *blades*, that are rotated about the k-space center, and allows motion detection/correction [16]. Each blade can be rapidly acquired using (3D-)EPI, yielding a fast, motion robust acquisition with low distortion [17]. **SPIRAL** trajectories are extremely efficient, and evenly distribute undersampling to  $k_x-k_y$  axes for improved parallel imaging. Stack-of-spirals use phase encoding along  $k_z$  axis and provide SNR boost through 3D encoding. This allowed a whole brain acquisition at 1mm isotropic resolution in just 2.5min, with comparable SNR to that of a 20min 3D-GRE [18].

*iii*) **Echo-shift:** exploits the unused time before the long TE to encode different subsets of the FOV. These subsets can be chosen as contiguous slabs [19] or as comb-shaped slices in **FIG3** which eliminate slab boundary artifacts. This also facilitates parallel imaging since a comb slice group spans the entire FOV along  $z$ , improving the distance between aliasing voxels [20].



**DISCUSSION:** While EPI is very efficient, achieving high resolution is difficult due to  $T_2^*$  blurring during the long echo train. Segmented EPI or 3D-GRE would be more suitable for such applications, while sacrificing some acquisition efficiency. EPI also suffers from  $B_0$ -related distortion, which can be mitigated by segmented acquisition, higher in-plane acceleration, or post-processing. Spiral trajectories are similarly efficient, but require more involved non-Cartesian reconstruction.  $B_0$  artifacts in spiral acquisition manifest as blurring rather than distortion, and can be mitigated by incorporating the field map in the reconstruction [21], or by a segmented (multi-shot) approach. On the other hand, echo-shift is more suitable for GRE readout rather than EPI or spiral encoding since GRE acquisitions have more dead time. Echo-shift is especially useful for phase imaging since it minimizes unused time while achieving long TE, and can be combined with parallel imaging for  $>20\times$  acceleration [22].

**REFERENCES:** 1] T Liu MRM09; 2] C Liu MRM10; 3] M Griswold MRM02; 4] D Khabipova NIMG15; 5] K Pruessmann MRM09; 6] X Li NIMG12; 7] F Breuer MRM06; 8] B Bilgic MRM15; 9] S Cauley ISMRM16; 10] H Sun MRM15; 11] K Setsompop MRM12; 12] C Langkammer NIMG15; 13] P Sati MSJ14; 14] B Poser ISMRM14; 15] M Narsude MRM15; 16] J Pipe MRM99; 17] S Holdsworth JMIR15; 18] B Wu NIMG12; 19] Y Ma MRM16; 20] H Ye ISMRM16; 21] B Sutton TMI03; 22] B Bilgic ISMRM16